# Radiogenic whole-rock lead in Precambrian metasedimentary gneisses from South Norway: evidence of Sveconorwegian LILE mobility

TOM ANDERSEN & INGRID ANNE MUNZ

Andersen, T. & Munz, I. A.: Radiogenic whole-rock lead in Precambrian metasedimentary gneisses from South Norway: evidence of Sveconorwegian LILE mobility. *Norsk Geologisk Tidsskrift*. Vol. 75, pp. 156–168. Oslo 1995. ISSN 0029-196X.

Present-day whole-rock lead isotopic compositions of Precambrian metasedimentary rocks from the Sveconorwegian province of South Norway have been determined by mass spectrometry. The $^{206}Pb/^{204}Pb$ ratio ranges from 17.208 to 122.4 for the 39 samples analysed, most samples having $^{206}Pb/^{204}Pb \geqslant 21$. The samples show an imperfect fit to a regional uranogenic lead correlation line ('scatterchron') with an age of $1131 \pm 30$ Ma, and also some correlation of $^{208}Pb/^{204}Pb$ with $^{206}Pb/^{204}Pb$. The metasediments must have accumulated radiogenic lead at high to very high U/Pb ratios since the Precambrian ($^{238}U/^{204}Pb \geqslant 24$). The linear correlation of uranogenic lead isotope ratios is due to the introduction of uranium to the mestasediments during the Sveconorwegian orogeny, most probably as a result of interaction with fluids of crustal origin in amphibolite facies metamorphic conditions. The strong differentiation of the U/Pb ratio brought about by this process overshadowed any residual heterogeneity in the initial isotopic composition of lead in the rocks on a regional scale. Prior to uranium introduction, the precursors of the rocks studied had evolved in a LILE-enriched 'upper continental crust' environment for several hundred million years. If a crustal residence age of the protolith in the range 1700–1900 Ma is assumed (in accordance with published depleted mantle neodymium isotope model ages on these and related rocks), the average $^{238}U/^{204}Pb$ ratio of the precursor would be in the range 20–24.

*T. Andersen, Laboratory of Isotope Geology, Mineralogisk-Geologisk Museum, Sars gate 1, N-0562 Oslo, Norway;*
*I. A. Munz, Institute for Energy Technology, P.O. Box 40, N-2007 Kjeller, Norway*

## Introduction

The processes of erosion and deposition of clastic material tend to average out compositional heterogeneities in the source terrane, making clastic (meta) sediments representative of the composition of large-scale domains of the continental crust (Taylor & McLennan 1985). Deviations from reasonable 'average upper continental crust' values in trace element concentrations patterns, or in the ratios of radiogenic isotopes in such rocks, are therefore indicators of open-system processes which have differentiated these elements during or after deposition of the sediments. Because the isotopic composition of lead changes by accumulation of radiogenic $^{206}Pb$, $^{207}Pb$ and $^{208}Pb$, which are the final decay products of radioactive U and Th isotopes, the present-day isotopic composition of lead in clastic metasediments is a powerful indicator of processes in the geological past involving mobility of U, Th and Pb, all of which are large ion lithophile elements (LILE).

Several studies have suggested that LILE and other trace components were mobilized by metamorphic fluids in parts of the Precambrian continental crust of South Norway during the Sveconorwegian orogeny at 1.25–0.9 Ga. Processes which have been recognized include LILE and chalcophile element depletion related to granulite-facies metamorphism (Field et al. 1980; Smalley et al. 1983; Cameron 1989a, b; Cameron et al. 1993), as well as albitization and other metasomatic processes at lower grade of metamorphism (e.g. Field et al. 1985; Cameron 1993), in which elements commonly considered immobile during crustal metamorphism (e.g. LREE) have been mobilized (Munz et al. 1994). So far, few lead isotope data with a direct bearing on Precambrian LILE mobilization have been published from South Norway, except data on lead ore deposits (Moorbath & Vokes 1963). In the present article, the Pb isotope systematics of suites of metasedimentary rocks from the Bamble and Kongsberg sectors of South Norway are presented, and their bearing on LILE mobilization and the crustal pre-history in the area is discussed.

## Geological setting

The continental crust of South Norway (Fig 1) is part of the Southwest Scandinavian Domain of the Baltic Shield (Gaál & Gorbatschev 1987), and has a complex and not fully understood evolutionary history in the Precambrian. In the south and central parts of the Baltic Shield, orogenic events are recognized at 1.75–1.9 Ga (Svecofennian), at ca. 1.5 Ga (Gothian or Kongsbergian) and at 1.2–0.9 ga (Sveconorwegian) (Gaál & Gorbatschev 1987; Gorbatschev & Bogdanova 1993). In South Norway, there is no undisputed record of rocks older than ca. 1.6 Ga (O'Nions & Baadsgaard 1971; Jacobsen & Heier 1978; see De Haas et al. 1993 for an alternative view), but ample evidence of magmatism and high-grade metamorphism in the Sveconorwegian (e.g. Munz & Morvik

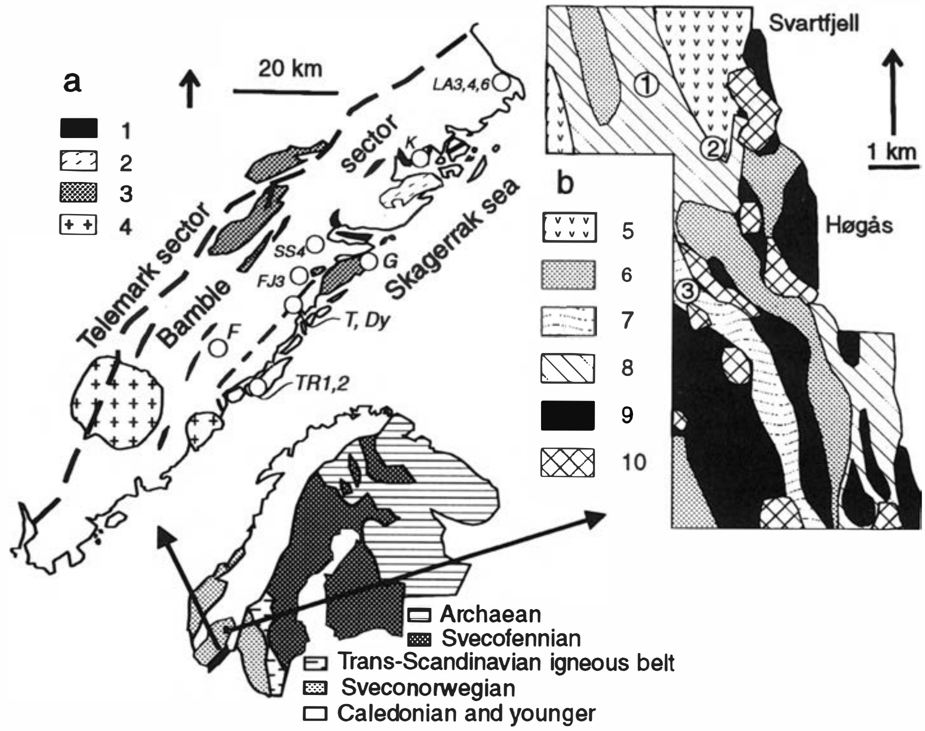


*Fig. 1.* (a) *The Bamble sector.* Circles represent sampling localities, identified by sample name or by locality indicator as in Table 1. Geological units: 1 = Gabbro and metagabbro, 2 = Levang gneiss dome, 3 = syntectonic charnockitic intrusions, 4 = Post-tectonic granites (Grimstad and Herefoss). Metasediments have been left blank. *Heavy, broken line*: Porsgrunn–Kristiansand shear zone, separating the Bamble and Telemark sectors. *Thin, dash-dot line*: Granulite-facies isograd around Arendal; granulite-facies rocks occur SE of the line. (b) *The Modum complex.* Localities 1, 2 and 3 refer to sampling localities in Table 1. The Tingelstadtjern, Sporpin, Kaggefoss and Embretsfoss localities are outside the area of the map. Rock units: 5 = granitic and dioritic gneiss, 6 = quartzite, 7 = micaschist, 8 = nodular gneiss, 9 = metagabbro/amphibolite, 10 = albite-rich rocks.

1991; Kullerud & Machado 1991; Dahlgren et al. 1990a, b; Kullerud & Dahlgren 1993; De Haas et al. 1993; Heaman & Smalley 1994). However, metasediments from the Bamble and Kongsberg sectors of South Norway (Fig. 1) show depleted mantle Nd model ages (DePaolo 1981 model) of 1.7 to 1.9 Ga, which indicates that their average protoliths have resided in the continental crust since the Svecofennian period (Andersen et al. 1995; Munz et al. 1994).

The material of the present study comes from the Modum complex in the northernmost part of the Kongsberg sector and from several localites within the Bamble sector of South Norway (Fig. 1). The Bamble sector consists mainly of supracrustal gneisses (including metapelites and metasemipelites), quartzites and amphibolites, penetrated by gabbroic to granitic intrusions, some of which are syn-tectonic. Several syn-tectonic intrusions have high-grade mineralogy (such as charnockitic augen gneisses and enderbitic gneiss; Touret 1969; Starmer 1985). In the Kongsberg sector amphibolite-facies gneisses of tonalitic to granodioritic composition are dominant lithologies (Bugge 1936, 1937; Jacobsen & Heier 1978). In the Modum complex, supracrustal rocks similar to those of the Bamble sector are abundant. The Kongsberg sector may be a downfaulted block which belongs tectonically to the late Palaeozoic Oslo Rift (Sundvoll & Larsen 1993).

The bulk of the Bamble and Kongsberg sectors have reached metamorphic grades of middle to upper amphilbolite facies. Granulite-facies rocks are only found in restricted areas, such as the coastal area of the Bamble sector near Arendal (Fig. 1), in contact aureoles around some charnockitic intrusions (Hagelia 1989) and in restricted parts of the Kongsberg sector (Jacobsen & Heier 1978). In the Bamble sector, metamorphic temperatures above 800° have been found in both granulite-facies and amphibolite-facies areas (Touret 1971a; Nijland 1993). The regional transition from amphibolite to granulite facies when approaching the coast in the Bamble sector is most likely due to a combination of increasing temperature and change from a water-dominated to a $CO_2$ dominated metamorphic fluid regime (Touret 1971b, 1985; Nijland 1993, T.-L Knudsen pers. comm 1995). Other occurrences of granulite-facies rocks in the Bamble sector may be due to contact metamorphism (Hagelia 1989); these have not been sampled in the present study. There is no evidence of granulite-facies metamorphism in the Modum complex.

## The material studied

The samples of the present study have been selected to cover as wide as possible a range of lithologies of documented or assumed metasedimentary character. Although the Kongsberg and Bamble sectors are now separated by the Oslo Graben, the two sectors most probably represented a continuous terrane in the Precambrian (A. Bugge 1936; J. A. W. Bugge 1943; Jøsang 1966; Starmer 1976). The correlation between the two sectors is largely based on the similarities between the metasedimentary sequences. The samples in this study are thus assumed to have experienced similar geological histories.

*Table 1.* Lead isotope analyses, U and Pb concentrations and calculated parameters.

| | Locality on map (where different from sample name) | Rock type | $^{206}Pb/^{204}Pb$ | $^{207}Pb/^{204}Pb$ | $^{208}Pb/^{204}Pb$ | Calculated $\mu_2$ | Calculated change of U/Pb, % | Actual concentrations, ppm | |
|---|---|---|---|---|---|---|---|---|---|
| | | | | | | | | Pb | U |
| *Metasediments, Bamble sector* | | | | | | | | | |
| 89120 | G | Metapelite | 20.232 | 15.786 | 42.024 | 21 | −12 | | |
| 89121 | G | Metapelite | 17.208 | 15.459 | 37.257 | 6 | −75 | | |
| 89123 | G | Graphite rich metapelite | 18.367 | 15.622 | 37.212 | 11 | −52 | | |
| KI-Q1 | F | Quartzite | 25.672 | 16.249 | 44.922 | 49 | 104 | | |
| KI-Q2 | F | Quartzite | 30.020 | 16.586 | 49.354 | 72 | 199 | | |
| BS 53 | K | Quartzite | 21.331 | 15.790 | 45.451 | 27 | 14 | | |
| BS 55 | K | Metasemipelite | 21.288 | 15.766 | 43.011 | 27 | 14 | | |
| BS 57 | K | Quartzite | 21.418 | 15.818 | 43.393 | 28 | 15 | | |
| BS 60 | K | Metapelite | 24.654 | 16.096 | 47.204 | 44 | 85 | | |
| *Cordierite-bearing rocks, Bamble sector* | | | | | | | | | |
| SS4 | | Cordierite–garnet–orthoamphibole gneiss | 48.216 | 17.939 | 87.431 | 167 | 596 | | |
| LA3 | | Cordierite–orthoamphibole gneiss | 31.807 | 16.828 | 63.372 | 80 | 234 | 7 | 1 |
| LA4 | | Cordierite–orthoamphibole gneiss | 122.413 | 23.684 | 146.389 | 554 | 2208 | 3 | 4 |
| LA6 | | Cordierite–orthoamphibole gneiss | 33.813 | 16.797 | 64.588 | 92 | 284 | 5 | 1 |
| FJ3 | | Cordierite–orthoamphibole gneiss | 42.493 | 17.405 | 75.124 | 138 | 475 | | |
| DY | | Garnet-sillimanite–quartz gneiss | 24.967 | 16.177 | 48.099 | 46 | 90 | | |
| TR1 | | Cordierite–orthopyroxene gneiss | 20.561 | 15.761 | 37.456 | 23 | −4 | 1 | 1 |
| TR2 | | Cordierite–orthoamphibole gneiss | 21.416 | 15.822 | 41.415 | 28 | 15 | 5 | 1 |
| *Metasediments, Modum Complex (Kongsberg sector)* | | | | | | | | | |
| M 2A | 1 | Nodular gneiss | 26.901 | 16.301 | 52.001 | 56 | 133 | | |
| M 2B | 1 | Nodular gneiss | 28.331 | 16.387 | 52.978 | 63 | 164 | | |
| M 3 | 1 | Nodular gneiss | 30.673 | 16.608 | 55.950 | 75 | 214 | | |
| M 4 | 1 | Nodular gneiss | 25.798 | 16.176 | 49.800 | 50 | 110 | | |
| M 5 | 1 | Nodular gneiss | 29.952 | 16.500 | 56.616 | 72 | 200 | | |
| M 7 | 1 | Neosome in nodular gneiss | 45.130 | 17.680 | 81.016 | 151 | 530 | | |
| IA81 | 2 | Nodular gneiss | 48.251 | 17.852 | 54.839 | 168 | 599 | | |
| NG | 1 | Nodular gneiss composite | 28.661 | 16.489 | 53.121 | 65 | 169 | 6 | 3 |
| GG | 1 | Granitic gneiss composite | 29.056 | 16.538 | 50.850 | 67 | 177 | | |
| SP3B | Sporpin | Biotite schist | 37.803 | 17.192 | 48.405 | 112 | 368 | 4 | 2 |
| IA124 | Kaggefoss | Biotite schist | 27.964 | 16.368 | 54.061 | 61 | 156 | 4 | 1 |
| IA126 | | Biotite schist | 30.043 | 16.570 | 62.168 | 72 | 200 | 4 | 1 |
| IA116 | Embretsfoss | Biotite schist | 26.567 | 16.242 | 51.843 | 54 | 126 | 4 | 2 |
| IA620 | Embretsfoss | Magnesian micaschist | 25.522 | 16.172 | 59.827 | 49 | 103 | 2 | 1 |
| IA621 | Embretsfoss | Magnesian micaschist | 27.671 | 16.397 | 76.984 | 60 | 148 | 3 | 1 |
| IA622 | Embretsfoss | Magnesian micaschist | 30.776 | 16.536 | 93.343 | 77 | 219 | 2 | n/d |
| IA623 | Embretsfoss | Magnesian micaschist | 24.804 | 16.096 | 55.401 | 57 | 137 | 5 | 2 |
| IA37 | Tingelstadtjern | Magnesian micaschist | 23.798 | 16.105 | 62.230 | 39 | 64 | 1 | 1 |
| IA228 | 3 | Whiteschist | 20.713 | 15.830 | 54.854 | 23 | −2 | | |
| SpM1 | Sporpin | Marble | 37.568 | 17.100 | 54.862 | 112 | 365 | 3 | n/d |
| SpM3 | Sporpin | Marble | 27.192 | 16.418 | 49.706 | 57 | 136 | 2 | 1 |
| IA185 | Sporpin | Calc-silicate | 43.946 | 17.628 | 62.144 | 145 | 503 | 5 | 1 |

Analytical uncertainty, based on repeated runs of the NBS 981 common lead standard: ±0.15%. Model $\mu_2$ is calculated from a two-stage model of global lead isotopic evolution, as described in the text, relative to an age of 1131 Ma. U and Pb concentrations have been determined by XRF. n.d. = not detected, i.e. below the detection limit of the instrument. The calculated change in U/Pb is based on an assumed $^{238}U/^{204}Pb$ ratio of 24 immediately before U/Pb differentiation at 1131 Ma. Sporpin, Kaggefoss, Embretsfoss and Tingelstadtjern in the Modum complex are outside the map area of Fig. 1; a detailed map of the Embretsfoss locality can be found in Munz et al. (1994). Locality abbreviations (indicated in Fig. 1): G = Gjeving, K = Kragerø, F = Froland. XRF U and Pb concentrations are close to the detection limit, and should be regarded as semiquantitative.

### *Clastic metasediments*

Pb-Pb data on a suite of *quartzites* and *sillimanite gneisses* from the Froland and Hisøy area in the Bamble sector have been presented by Andersen et al. (1995); the reader is referred to this article for petrographic details and analytical data. Those data have been supplemented by analyses of two additional samples of quartzite from Froland (KI-Q1, KI-Q2), three samples of metapelitic gneisses from the Tvedestrand–Gjeving area (89120, 89121, 89123) and four samples from Kragerø (BS53, BS55, BS57, BS60), ranging from quartzite to metapelite (Table 1).

The metasediments of the Modum complex are dominantly of a clastic origin, i.e. quartzites and a variety of micaceous and feldspathic gneisses. However, a thin unit of marble with interlayered calc-silicate rocks is also present (below). Sedimentary precursors have also been suggested for altered rock-types like orthoamphibole–cordierite rocks and whiteschists (Munz 1990) and of magnesite–serpentinite deposits (Jøsang 1966; Petrascheck 1971).

The characteristic feature of *nodular gneisses* is nodules of quartz and sillimanite. The matrix ranges from quartzitic, quartz-micaceous to granitic composition. The nodules form an axial planar foliation. Migmatites of granitic composition are frequent. More extensive descriptions of nodular gneisses from the Modum complex and from the Bamble Sector are given by Brøgger (1934), Elliot & Morton (1965), Jøsang (1966), Munz (1986) and Nijland et al. (1993). The samples of nodular gneiss represented in this study are mainly of granitic composition. Samples M2–M7 are collected at a single locality, M2–M6 are paleosomes consisting of quartz, K-feldspar, plagioclase, biotite and sillimanite, M7 a granitic neosome. Sample IA81 is a more quartz-rich type containing a small neosome. The NG and GG samples are composites of the nodular gneiss samples (neosomes excluded) and of granitic gneiss samples devoid of nodules in the northernmost part of the Modum complex, respectively.

In addition to the micaceous type of the nodular gneiss, several types of *micaschists* are present in the Modum Complex. A micaschist, which was described as quartz–phlogopite–hematite schist by Jøsang (1966), is an unusual Mg-rich type, commonly carrying intergrowths of talc and kyanite (Munz 1990). This micaschist locality contains domains of whiteschists, which are free of mica (Munz 1990). Samples IA37 and IA620–IA623 are representatives of this micaschist, also carrying talc and kyanite. Samples IA228 is a whiteschist. A more Fe-rich micaschist, containing biotite and occasionally garnet, is also present within the area (samples SP3, IA124, IA126 and IA116). Sample SP3B is collected from a micaschist zone within the Sporpin marble (below).The samples show an upper amphibolite facies mineralogy. The retrogradation is mainly limited to minor chloritization of the biotite and some muscovite alteration of the sillimanite nodules.

### *Marble*

The Sporpin Marble from the Modum complex is a sequence of interlayered calcite marbles, calc-silicate rocks and micaschists, cropping out over an area of ca. 100–200 m by 800 m. The marble layers consist of coarse-grained calcite and graphite. The calc-silicate layers commonly contain diopside, tremolite, calcite, quartz, K-feldspar, sphene and scapolite. Samples SpM1 and SpM3 are marbles, whereas IA185 is a calc-silicate rock.

### *Cordierite-bearing rocks*

In the Bamble sector, cordierite-bearing rocks occur as minor lenses and pods, mainly in metasedimentary gneisses (e.g. Touret 1969; Visser 1993; Kihle 1989; Kihle & Bucher-Nurminen 1992). Eight samples from six different localities in the Bamble sector have been analysed, three of which (LA3, 4 and 6) come from a single locality. The rocks range from cordierite-bearing metapelites (e.g. cordierite-bearing quartz-sillimanite gneiss), of an undisputed metasedimentary origin, to cordierite–orthoamphibole and cordierite–orthopyroxene rocks, whose protoliths may have been affected by metasomatic processes. All except the two samples from Tromøy (TR 1, 2) occur interlayered with metasedimentary gneisses supporting a supracrustal origin. The two cordierite–orthopyroxene rocks from Tromøy are associated with enderbitic gneisses and orthopyroxene-bearing amphibolites, and occur within the zone of maximum LILE depletion (Field et al. 1980); the nature of the protolith of these rocks is uncertain.

The mineralogy and metamorphic petrology of the Bamble cordierite-bearing rocks has been dealt with by e.g. Kihle (1989), Kihle & Bucher-Nurminen (1992), Thijssen & Maijer (1990) and Visser (1993).

## Pb-isotope data

### *Analytical method*

Lead was separated from powdered whole-rock samples by a standard anion-exchange method, using highly purified reagents and disposable minature HBr-HCl columns. Pb was loaded on single Re filaments by the silica gel–phosphoric acid method, and analysed in a Finnigan MAT 262 multicollector mass spectrometer in the static mode. The raw data were corrected for −0.11%/amu mass fractionation off-line; the fractionation was determined by multiple analyses of the NBS SRM 981 Pb standard. The total blank of the method was 0.3 to 0.5 ng. The reproducibility estimated from repeated analyses of the NBS 981 standard is better than ±0.15% ($2\sigma$).

$^{207}Pb/^{204}Pb$ vs. $^{206}Pb/^{204}Pb$ correlations were calculated using the ISOPLOT 2.57 software package (Ludwig 1986), using assigned $2\sigma$ errors (reproducibility + fractionation) of 0.2%. An error correlation coefficient of 0.6 and weighting proportional to the inverse square of the analytical error was initially assumed, but correlations for datasets with elevated MSWD ( > 3) are calculated using model 2 of Ludwig (1986), in which equal weight and zero error correlation is assigned to each point. Errors on age estimates are given as 95% confidence limits.

The U and Pb concentrations of selected samples were determined by XRF, using pressed powder pellets. Concentrations of a few parts per million of these elements must be regarded as semiquantitative.

### *Results*

New whole-rock lead isotope data on 39 samples are given in Table 1. In the subsequent discussion, these data are combined with additional, published data on metasedimentary rocks (quartzites and sillimanite-bearing gneisses) from Hisøy and Froland in the Bamble sector (Andersen et al. 1995), on galenas from late Palaeozoic sulphide deposits in the Bamble and Kongsberg sectors (Bjørlykke et al. 1990), and on a composite sample assumed to represent an average of the 'upper crust' in the southeastern part of the Telemark sector (Andersen & Taylor 1988).

The samples show a wide range of present-day isotopic composition, and a strong tendency towards radiogenic to extremely radiogenic values. Only two whole-rock samples have $^{206}Pb/^{204}Pb$ ratios lower than 20; the majority of whole-rock samples range from ca. 21 to extreme values. The quartzites and associated metapelites from

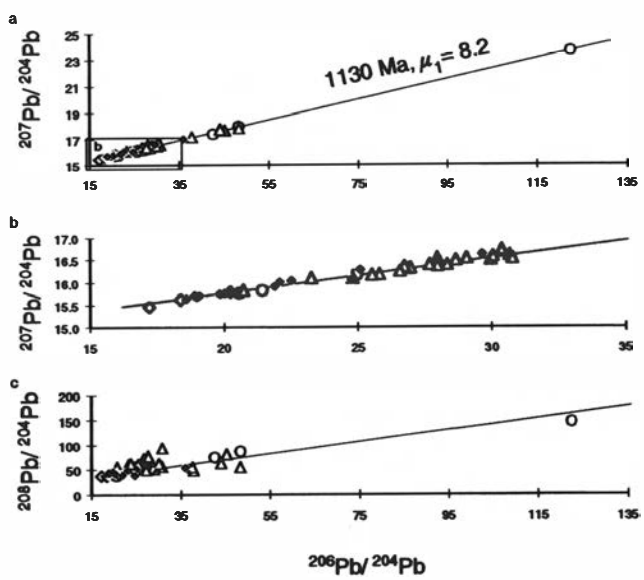


*Fig. 2.* Lead isotope correlation diagrams. Sample symbols: *Open circles* = Cordierite-bearing rocks, Bamble sector; *open triangles* = metasedimentary rocks, Modum complex; *rhombs* = quartzites and metasedimentary gneisses, Bamble sector (*open* = data from Table 1, *filled* = data from Andersen et al. 1995). (a) Uranogenic lead. The box indicates the detail blown up in (b). The line is a 1131 Ma isochron with single-stage model $\mu_1 = 8.20$. (b) Detail of (a). (c) Thorogenic lead. The reference line has an age of 1130 Ma, $\mu_1 = 8.20$ and Th/U = 4.

the Bamble sector both show the least radiogenic lead compositions (Fig. 2b) and the smallest range of variation, up to a $^{206}Pb/^{204}Pb$ ratio of ca. 35, when the samples of Andersen et al. (1995) are included (Fig. 2a). The maximum $^{206}Pb/^{204}Pb$ value recorded from micaschists from the Modum area is ca. 37. whereas both the quartz–sillimanite gneisses from Modum and the cordierite-bearing rocks from Bamble range up to ca. 50, but for one extreme cordierite rock (LA 4), which has a $^{206}Pb/^{204}Pb$ ratio of 122. It should be noted that this extreme value is not representative of that particular occurrence as a whole, as the other two samples from the same locality (LA 3, LA 6) give $^{206}Pb/^{204}Pb$ ratios of ca. 31 and ca. 33, respectively. The extremely radiogenic compositon of LA 4 must be due to heterogeneously distributed U-rich mineralization at this locality. It should be noted that the two samples of cordierite–orthopyroxene rock from within the zone of assumed maximum LILE depletion give $^{206}Pb/^{204}Pb$ ratios above 20.0, which does not agree with U depleted LILE distribution in these rocks since the Sveconorwegian metamorphism.

The data show pronounced linear correlation in the $^{207}Pb/^{204}Pb$ vs. $^{206}Pb/^{204}Pb$ diagram (Fig. 2a, b). Regression of all whole-rock samples from the Bamble sector and the Modum area together yields a correlation line ('scatterchron') with a Sveconorwegian age (1131 ± 30 Ma) and an elevated MSWD (17.3). The single-stage model $\mu_1$ value of the correlation line is $8.20 \pm 0.02$; see introduction to model $\mu_1$ and further discussion of its significance below. The actual age of this line is, of course, strongly controlled by the single sample with $^{206}Pb/^{204}Pb$ above 100. However, if regressed separately, the metasedimentary rocks from the Modum area, the cordierite-bearing rocks from Bamble and the quartzites and metapelites from the Hisøy and Froland areas all yield Sveconorwegian ages with overlapping errors and single stage model $\mu_1$ values; MSWD remains high for each of the sub-groups (Table 2). The metasediments from the Gjeving–Kragerø area also suggest a Sveconorwegian age, but with a very large uncertainty (1220 ± 450 Ma). The age and model $\mu_1$ value derived from the overall correlation line are therefore used in subsequent discussions. The significance of the age will be further discussed below. The correlation between $^{208}Pb/^{204}Pb$ and $^{206}Pb/^{204}Pb$ is much poorer, although the samples which are highest in uranogenic lead also have high $^{208}Pb/^{204}Pb$ (Fig. 2c). A 1131 Ma reference line with model $\mu_1 = 8.2$ and U/Th = 4 is shown in Fig. 2c.

The analysed Pb concentrations listed in Table 1 are lower than the average values of the upper continental crust (20 ppm; Taylor & McLennan 1985), whereas the uranium concentrations straddle the upper crustal average (2.8 ppm; Taylor & McLennan 1985). Actual U/Pb ratios range from an order of magnitude higher than the upper crustal average (0.4; Taylor & McLennan 1985) to much lower values. It should be noted that uranium may be removed from the rock by recent, surface-near weathering processes, and that the concentration and U/Pb

*Table 2.* Pb isotope correlation data.

| | Age (Ma) | $2\sigma$ (Ma) | MSWD | Model $\mu_1$ |
|---|---|---|---|---|
| All samples | 1131 | 30 | 17.3 | 8.2 |
| Modum | 1060 | 73 | 3.27 | 8.22 |
| Bamble cordierite-bearing rocks | 1137 | 40 | 10.1 | 8.12 |
| Hisøy and Froland metasediments | 1262 | 110 | 1520 | 8.18 |
| Gjeving-Kragerø metasediments | 1220 | 450 | 8.8 | 8.09 |

The data from the Hisøy–Froland metasediments are from Andersen et al. (1995); all other calculations have been made using Pb-isotope data given in Table 1.

ratio determined today need not to be representative of the composition of the rocks since the Precambrian (e.g. Rosholt & Noble 1969; Rosholt et al. 1973).

## Modelling of the U/Pb system

### *Principles*

The present-day Pb isotopic composition of a system (mineral, whole-rock sample, crustal reservoir) reflects its age (i.e. the time that has passed since the final isotopic homogenization of Pb) and U–Th–Pb chemistry, as well as the history and compositional characteristics of its source (e.g. Gale & Mussett 1973; Zartman & Doe 1981; Faure 1986). The existence of two parallel uranogenic decay series ($^{238}U$-$^{206}Pb$ and $^{235}U$–$^{207}Pb$) and the related $^{232}Th$-$^{208}Pb$ series makes the U-Th-Pb system a sensitive indicator of multi-stage processes. A lucid and non-technical introduciton to the interpretation of multi-stage leads is given by Faure (1977, pp. 249–263).

For a system accumulating radiogenic lead isotopes in a closed reservoir with constant $^{238}U/^{204}Pb$ ($\mu_i$) from the time $t_{i-1}$ to $t_i$, the isotopic evolution of Pb is given by the decay equations of $^{235}U$, $^{238}U$ and $^{232}Th$ (Gale & Mussett 1973);

$$^{206}Pb/^{204}Pb = \alpha + \mu_i(e^{\lambda_{238}t_{i-1}} - e^{\lambda_{238}t_i}) \quad \text{(i)}$$

$$^{207}Pb/^{204}Pb = \beta + (\mu_i/137.88)(e^{\lambda_{235}t_{i-1}} - e^{\lambda_{235}t_i}) \quad \text{(ii)}$$

$$^{208}Pb/^{204}Pb = \gamma + k_i\mu_i(e^{\lambda_{232}t_{i-1}} - e^{\lambda_{232}t_i}) \quad \text{(iii)}$$

where $\lambda_A$ is the decay constant for the relevant radioactive parent isotope, $i_{i-1}$ is the time at which closed-system evolution started in the reservoir, $\mu_i$ is the $^{238}U/^{204}Pb$ ratio, $k_i$ is the $^{232}Th/^{238}U$ ratio and $\alpha$, $\beta$ and $\gamma$ are the respective initial Pb isotope ratios at $t_{i-1}$. If evolution has taken place in several, subsequent stages at different $\mu_i$-values, the total result will be a sum of the evolution at each stage, e.g.:

$$^{206}Pb/^{204}Pb = \alpha + \sum_{i=1}^{n} \mu_i(e^{\lambda_{238}t_{i-1}} - e^{\lambda_{238}t_i}) \quad \text{(iv)}$$

and similar for the other parent–daughter systems.

Previous lead isotope studies in the Precambrian of South Norway have shown that at least three subsequent stages of evolution are needed to account for the lead isotope variations in Sveconorwegian metamorphic rocks (Andersen et al. 1994, 1995). In the present study, a less complex two-stage model is adopted, which accounts for the Sveconorwegian U–Th–Pb fractioning history, but gives less information on the evolution of the crustal precursor(s).

In a two-stage system whose start- and end-points are known or constrained by independent data, $\mu_1$ and $\mu_2$ are univariant functions of the age of the intermediate isotopic homogenization event ($t_1$). In the present model, the first stage starts from meteoritic lead at $t_0 = 4.57$ Ga (the 'age of the earth'). The model is further constrained by $n = 2$, $t_1 = 1.13$ Ga (Table 2) and $t_2 = 0$. For the evolution of the $^{206}Pb/^{204}Pb$ ratio with time, equation (iv) then simplifies to:

$$^{206}Pb/^{204}Pb = \alpha_0 + \mu_1(e^{\lambda_{238}t_0} - e^{\lambda_{238}t_1}) + \mu_2(e^{\lambda_{238}t_1} - 1) \quad \text{(v)}$$

and for the $^{207}Pb/^{204}Pb$ ratio:

$$^{207}Pb/^{204}Pb = \beta_0 + [\mu_1(e^{\lambda_{235}t_0} - e^{\lambda_{235}t_1}) + \mu_2(e^{\lambda_{235}t_1})]/137.88 \quad \text{(vi)}$$

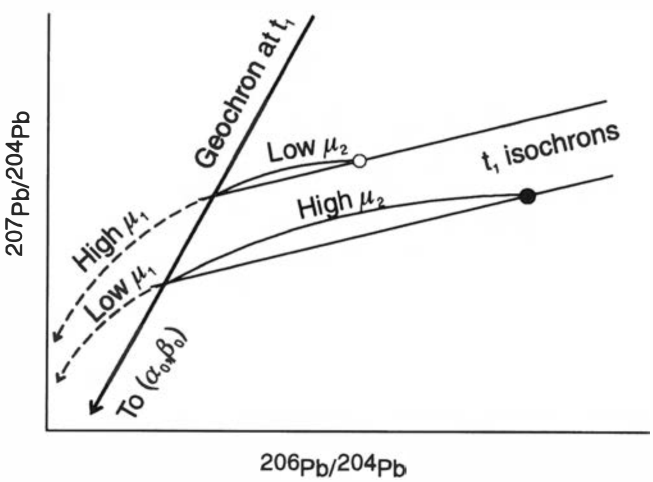


*Fig. 3.* A schematic view of a two-stage model for global lead isotopic evolution (e.g. Faure 1977). Global lead evolution is assumed to start from meteoritic lead at $t_0 = 4.57$ Ga. At $t_1$, all undisturbed systems will plot at the *geochron at* $t_1$, the positions of individual systems along the geochron depend upon the $^{238}U/^{204}Pb$ ratio (or $\mu_1$value) of each system during this first stage of evolution. Both the geochron at $t_1$ and the two first-stage growth curves (broken) start from a meteoritic initial lead composition ($\alpha_0$, $\beta_0$), which lies off the scale of the figure (indicated by arrows). The position of a two-stage system today depends also on the $^{238}U/^{204}Pb$ ratio since $t_1$ (or $\mu_2$value). The figure shows two present-day rock compositions (dots). If $t_1$ is known, unique $\mu_1$ and $\mu_2$ values may be calculated for each sample by solving equations (v) and (vi), or, graphically, by intersecting secondary isochrons through each present-day rock composition with the geochron at $t_1$. The two rock-lead compositions shown have been chosen to represent combinations of high $\mu_1$ and low $\mu_2$ and vice versa. The paths of these two rocks with time since $t_1$ are indicated by second-stage growth curves (curved, solid lines).

In equations (v) and (vi), $\alpha_0$ and $\beta_o$ represent the composition of meteoritic lead at $t_0 = 4.57$ Ga. Both $\mu_1$ and $\mu_2$ can be calculated for each individual sample by solving two simulataneous linear equations with two unknowns. Graphically, this can be explained as intersecting secondary model isochrons with age $t_1$ through each individual point in Fig. 2a, b with the geochron at $t_1$, as illustrated in Fig. 3. For a set of data defining an isochron or a more poorly fitted correlation line ('scatterchron'), the $\mu_1$ values obtained from the individual samples will, of course, average to the model $\mu_1$ derived from the best-fit line (Table 2), which is used in the subsequent discussion. Thus $\mu_1$ is a unique value, representing the time-integrated and area-integrated $^{238}U/^{204}Pb$ ratio of the crustal precursor of the rocks analysed, incorporating any intermediate stages and LILE exchange events from the formation of the Earth until the final U/Pb differentiation event at $t_1 = 1131$ Ma. Each sample is characterized by its individual $\mu_2$ value, which is the $^{238}U/^{204}Pb$ ratio required to produce its observed lead isotopic composition from a secondar initial defined by the intersection of the correlation line with the geochron at 1131 Ma (Fig. 3).

### *Sveconorwegian U/Pb differentiation*

The $\mu_2$ values obtained from the two-stage model vary from within the range usually assigned to LILE-enriched upper continental crust ($^{238}U/^{204}Pb$ = ca. 10–12), to extremely high values (Table 1, Fig. 3), which are uncommon in terrestrial whole rocks other than carbonates (Jahn & Cuvellier 1994).

Unlike the three-stage models used by Andersen et al. (1994, 1995), the present two-stage model gives no direct constraints on the age and composition on the immediate crustal precursor at 1131 Ma. However, if a reasonable fixed value for the $^{238}U/^{204}Pb$ ratio of the crustal protolith before U-Pb differentiation can be estimated, semi-quantitative calculation of the change (in percent or other relative units) in the U/Pb ratio at $t_1$ is possible. Andersen et al. (1994) estimated that the $^{238}U/^{204}Pb$ ratio for the crustal precursor of the Ubergsmoen augen gneiss averaged over its lifetime lay in the range 14–22, whereas the $^{238}U/^{204}Pb$ for the precursor of Froland and Hisøy clastic sediments was at least 18–30 (Andersen et al. 1995). In the present model, a $^{238}U/^{204}Pb$ ratio of 24 is adopted for crustal systems unaffected by Sveconorwegian U/Pb differentiation, and for the immediate precursor of rocks which have been influenced by this process. This assumption leads to conservative (i.e. minimum) estimates for the change in U/Pb ratio in the Svenconorwegian, compared to estimates based on average upper crustal $^{238}U/^{204}Pb$ ratios of 12 or less (e.g. Faure 1986; Zartman & Doe 1981), or on the minimum $\mu_2$s in Table 1. When recalculated to $t = 1131$ Ma, the Southeast Telemark crustal composite of Andersen & Taylor (1988) gives a $\mu_2$ value of 23.3 in the two-stage model, suggesting that a $^{238}U/^{204}Pb$ of 24 may indeed represent the average composition of at least some domains of the Precambrian upper continental crust of South Norway. It should be noted however, that the actual $\mu_2$ values obtained from some of the least radiogenic individual samples in the present dataset are less than 24 (Table 1).

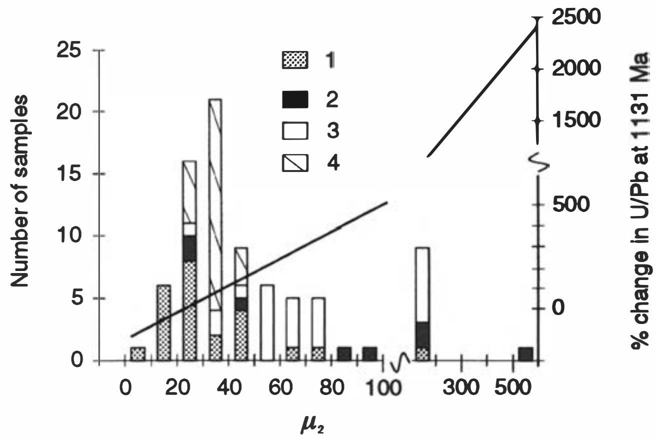


*Fig. 4.* The calculated post-Sveconorwegian $^{238}U/^{204}Pb$ ratio ($\mu_2$) in metasedimentary rocks and sulphide vein deposits from South Norway. Histogram signature: 1 = Quartzites and quartz–sillimanite gneisses from the Bamble sector, data from Table 1 and Andersen et al. (1995). 2 = Cordierite-bearing metapelites and cordierite–orthoamphibole/orthopyroxene rocks, Bamble sector (Table 1). 3 = Metasedimentary rocks, Modum complex, Kongsberg sector (Table 1). 4 = Lead in sulphides, 270 Ma vein deposits in the Bamble and Kongsberg sectors (data from Bjørlykke et al. 1990). The curve (right-hand scale) represents the change in the U/Pb ratio at 1131 Ma, assuming a $^{238}U/^{204}Pb$ ratio of 24 in the immediate precursor. Note break in scale at 500% change.

The calculated $\mu_2$ values and the changes in U/Pb in Svenconorwegian time implied by the modified two-stage model are illustrated in Fig. 4, and range from an apparent lowering of U/Pb in some of the quartzites and quartz-sillimanite gneisses from Bamble, to an increase in the vast majority of samples. Within each of the sample groups, U/Pb increases range from less than 50 to several hundred percent; the extremely highly radiogenic LA 4 (cordierite-bearing rock from Bamble) indicates an increase in U/Pb of more than 2200%. The numerical value of the change in U/Pb of course depends on the actual $^{238}U/^{204}Pb$ ratios assumed for the precursor. However, only unrealistically high $^{238}U/^{204}Pb$ ratios in the precursor ($\gg 24$) will significantly modify the pattern of U/Pb change illustrated in Fig. 4.

It is necessary to distinguish between the $\mu_2$ value calculated from Pb isotopic data, which is insensitive to recent weathering, and the measured, present-day U/Pb ratio. With the exception of LA 4, high $^{206}Pb/^{204}Pb$ is not correlated with high measured U/Pb (Fig. 5b), which is a strong indication that the samples have suffered some recent uranium loss or lead gain by surface weathering.

## Discussion

### *The geochronology of Sveconorwegian metamorphism*

The high-grade nature of Sveconorwegian metamorphism has now been documented by Sm-Nd and U–Pb

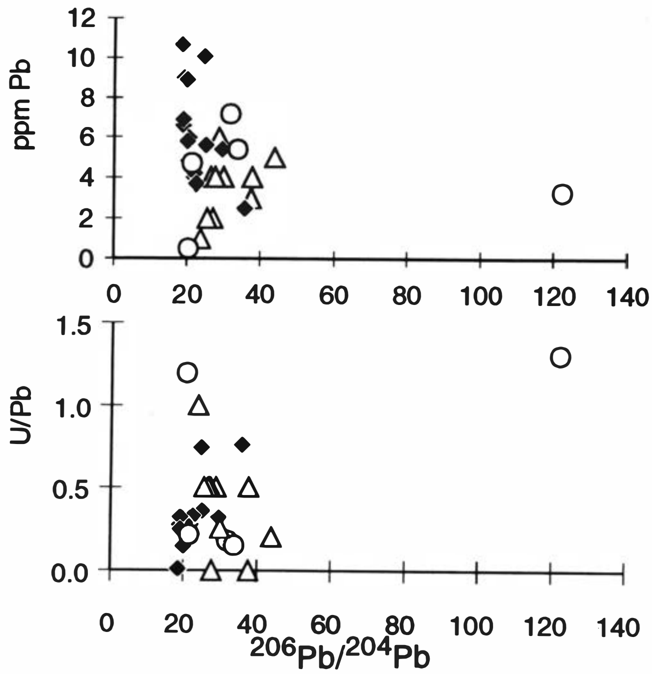


*Fig. 5.* Lack of correlation between present-day lead isotopic composition, lead contents and (analysed) U/Pb ratio. Sample symbols as in Fig. 2. Lead and uranium concentrations have been determined by XRF. Concentration data are given in Table 1, except for quartzites and metasedimentary gneisses from the Bamble sector (filled rhombs), which are from Knudsen et al. (in prep.).

geochronology on granulite parageneses, suggesting that granulite-facies metamorphism in the Bamble sector took place in the period 1100–1150 Ma (Kullerud & Machado 1991; Kullerud & Dahlgren 1993). This high-grade event was followed by lower-grade metamorphism (amphibolite facies to greenschist facies), evidence of which can be found in cross-cutting hydration veins within the high-grade terranes (Field et al. 1985; T.-L Knudsen, pers. comm. 1995). The Modum Complex has experienced several episodes of large-scale interaction between rocks and aqueous fluids, resulting in the formation of the high-grade metamorphic orthoamphibole–cordierite rocks and whiteschists and in extensive retrograde alteration (Munz 1990; Munz et al. 1994, 1995). At least two stages of albitization followed by an episode of carbonatization occurred in the area. The first stage of albitization has been dated by U–Pb on titanite to $1080 \pm 3$ Ma (Munz et al. 1994). The age of the later stages of fluid infiltration is not known. The metamorphic condition of this retrogradation is greenschist facies or lower. The P–T conditions of the latest stage of fluid infiltration resulting in quartz veins have been determined at 250–300°C and 1–2 kbar (Munz et al. 1995).

In the Bamble sector, the age of the secondary processes is less well established, but U–Pb data from titanites suggest low-grade reworking at ca. 1060 Ma (Heaman & Smalley 1994). A date of $1131 \pm 30$ Ma clearly postdates the emplacement ages of Sveconorwegian gabbros in the Modum complex (1224 Ma; Munz & Morvik 1991), but overlaps within error with ages for gabbro emplacement (1110–1232 Ga; Dahlgren et al. 1990b; De Haas et al. 1993), high-grade metamorphism (1100–1150 Ma; Kullerud & Dahlgren 1993) and emplacement of syntectonic granitic to monzonitic intrusions (1120–1150 Ma; Hagelia 1989; Kullerud 1991; Heaman & Smalley 1994) in the Bamble sector. When regressed alone, the metasediments from Modum yield an age of $1060 \pm 73$ Ma, with a moderate MSWD of 3.27 (Table 2). This date is indistinguishable from the age of the early albitization in the area. There is, however, no indication of an extensive low-temperature retrogradation of the present samples. Given the large error of the Pb-Pb age, the uranium mobilization probably took place at high-grade or early retrograde conditions, prior to the albitization event. The observation that the lead isotopic composition of a neosome in nodular gneiss (sample M7) is not significantly more radiogenic than the gneiss itself, indicates that the U/Pb differentiation post-dates migmatization, which was most probably related to the maximum metamorphic temperature.

## Significance of the Pb–Pb correlation

The samples analysed in the present study come from widely dispersed localities within rock complexes in which initial isotopic homogeneity of lead should not be expected, at least not over wide distances and across lithological boundaries. Nevertheless, regional correlation lines with apparently meaningful, Sveconorwegian ages may be calculated from the data. The age of deposition of the sediments studied here is not known with certainty, but it must certainly predate penetrating gabbroic intrusions with ages above 1200 Ma (Dahlgren et al. 1990b; Munz & Morvik 1991). Lead and strontium isotope data on the quartzites and quartz–sillimanite gneisses from Froland and Hisøy imply residence in a LILE-enriched 'upper crustal' environment for an extended period of time (at least 300–400 Ma) prior to sedimentation (Andersen et al. 1995). The Sveconorwegian ages reported here must therefore reflect U–Pb differentiation, possibly coupled with (partial) Pb isotopic homogenization by some process or processes after deposition of the sediments, rather than the age of the protolith.

Clastic metasediments may have elevated uranium–lead ratios because of the tendency of resistant heavy minerals like zircon and monazite to concentrate uranium. Even detrital quartz may have elevated U/Pb ratios, due to uranium incorporated into fluid or solid inclusions during its primary crystallization . As a consequence, clastic sediments may acquire highly radiogenic Pb isotopic compositions (Hemming et al. 1994). In systems affected only be mechanical processes (weathering, transport, deposition) and isochemical recrystallization, the Pb isotope systematics of whole rocks will reflect the age of crystallization of rocks within the crustal source terrane, rather than syn- and post-sedimentary processes (Hemming et al. 1994).

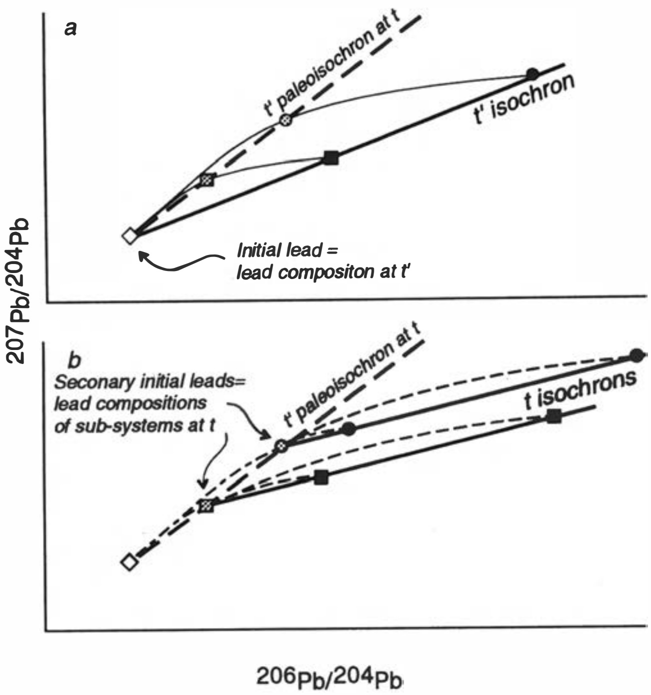


*Fig. 6.* Evolution of lead isotope composition in simple multi-stage systems, after Gale & Mussett (1973), Faure (1977) and Whitehouse (1989). The evolutionary sequences illustrated are mathematically similar to the global two-stage model in Fig. 3, differing only in that the starting-point is not necessarily equal to meteoritic lead at the age of the earth (hence the general terms $t$ and $t'$ are used rather than the $t_i$'s of the global model). (a) A simple system, with initial lead isotope homogenization and concurrent U–Pb differentiation at $t'$. The paleoisochron is the locus at $t(0 < t < t')$ of all points originating from a homogeneous initial lead at $t'$, whereas the $t'$ isochron is the locus of all such points today. Growth curves for two sub-systems are shown, as well as the positions of two samples at $t$ (shaded) and today (black). (b) A slightly more complex evolution, in which U is differentiated from Pb at $t$, without simultaneous isotopic homogenization of lead. The evolution from $t'$ until $t$ is equivalent to the case shown in (a) (growth curves shown as dash-dot curves). Immediately before the differentiation event, internally homogeneous systems differing in $^{238}U/^{204}Pb$ are aligned along the $t'$ paleoisochron at $t$ (shaded symbols). At $t$, uranium is introduced to individual rock volumes with no relationship to their lead isotopic composition at the time; from $t$ until the present each rock volume will evolve along its final-stage growth curve (shown as broken lines) according to its acquired $^{238}U/^{204}Pb$ ratio. Today, rock volumes having had the same lead isotopic composition at $t$ will plot along secondary isochrons (solid lines). Two such isochrons are shown in the figure.

A scenario in which a Pb–Pb isochron reflects crystallization of the source terrane ($t'$), rather than syn- or post-sedimentary processes is illustrated in Fig. 6a. In this idealized system, the lead isotopic composition was homogenized, and uranium was differentiated from lead at $t'$, after which different sub-systems (minerals, rock volumes) have retained constant U/Pb ratios until the present. A uranium-free system (galena, K-feldspar) will not accumulate radiogenic lead, and its composition has remained fixed in the diagram (white diamond). Systems with non-zero U/Pb will follow growth curves, characterized by constant $^{238}U/^{204}Pb$ (*squares*: moderate ratio, *circles*: high ratio). At present, the isotopic compositions are colinear with the initial lead along an isochron whose slope corresponds to $t'$. At an intermediate time, $t(t' > t > 0)$, the points were colinear along the $t'$ paleoisochron at $t$, as shown by the shaded symbols in Fig. 6a.

A different U–Pb scenario, in which the present-day lead isotope correlation may reflect the age of a U/Pb differentiation event at $t$ $(0 < t < t')$ is illustrated in Fig. 6b (corresponding to the type IIa U–Pb behaviour of Whitehouse 1989). This scenario is slightly more complex than the simple case in Fig. 6a, as an extra stage of radiogenic lead accumulation, following the U/Pb differentiation event must be taken into account. Starting from the same initial lead composition as in Fig. 6a at $t'$ lead evolves along growth curves equivalent to those of Fig. 6a until immediately before the U/Pb differentiation at $t$ (grey symbols aligned at the $t'$ paleoisochron at $t$ in Fig. 6b). At $t$, different amounts of uranium are added (or different amounts of lead removed) from individual rock volumes, with no predictable relationship to the lead isotopic composition at the time. From $t$ until the present, each rock volume will develop along its individual growth curve, depending on its actual $^{238}U/^{204}Pb$ ratio (a few examples are shown in Fig. 6b). Today, only samples which had identical lead isotopic composition at $t$ are colinear along an isochron with age $t$. Two final-stage isochrons are shown in Fig. 6b, corresponding to internally homogeneous precursors with moderate (squares) or high (circles) $^{238}U/^{204}Pb$ ratio from $t'$ until $t$. If enough uranium is introduced, so that the radiogenic lead accumulated since $t$ overshadows the overall difference in initial lead isotopic composition at $t$, a meaningful estimate of $t$ will be obtained from the entire dataset, although usually with a less-than-perfect-fit, expressed by an elevated MSWD, as is indeed seen in the present data. Such a scenario, in which the U/Pb was increased at $1131 \pm 30$ Ma, can adequately explain the distribution of lead isotope compositions in the metasedimentary rocks studied here. The imperfect correlation of the $^{208}Pb/^{204}Pb$ ratio with $^{206}Pb/^{204}Pb$ indicates that thorium to some extent followed uranium in this process, although there is no one-to-one relationship between the U/Pb and the Th/Pb ratios.

## LILE mobility in the Precambrian crust of South Norway

Strong differentiation of the U/Pb ratio without simultaneous homogenization of Pb may be brought about by the selective addition of U or by the removal of Pb. If lead loss was the controlling mechanism, selective removal of more than 80% of the initial lead content at constant U would be needed to account for present-day $^{206}Pb/^{204}Pb$ ratios above 40. Because of the tendency of Pb to be incorporated into potassium feldspar, regional lead-loss on the scale needed here is unlikely. On the other hand, uranium may be quite mobile in crustal fluids, which is reflected in the characteristic differences in its concentration between U-depleted 'lower crustal' granulites and complementary U-enriched rocks of the 'upper continental crust' (Lambert & Heier 1967; Zartman & Doe 1981). If lead-loss was the determining mechanism, a tendency towards inverse correlation of present-day lead isotopic composition and lead concentration should be expected. This is not observed in Fig. 5a, which shows that the most radiogenic samples show intermediate lead concentration. The Sveconorwegian increase of the U/Pb ratio seen in the present material is therefore more likely due to selective uranium introduction than to lead loss.

Uranium may have been introduced from seawater during deposition of the sediments, or during metamorphic fluid-rock interaction. Is is significant that the Sporpin marble from Modum overlaps with nodular gneisses and micaschists in lead composition; both its associated calc-silicate rocks and some of the samples of nodular gneiss are more radiogenic than the marble (Table 1). This is somewhat surprising, as many Precambrian marlbes show a tendency to extreme spread in U/Pb, yielding some of the most radiogenic present-day whole-rock lead compositions known from the terrestrial rocks (Jahn & Cuvellier 1994). Commonly, such marbles show a conspicuous lack of correlation of thorogenic and uranogenic lead, or a very flat correlation line in the $^{208}Pb/^{204}Pb$ vs $^{206}Pb/^{204}Pb$ diagram, which is thought to be due to selective introduction of U from seawater (Jahn & Cuvellier 1994). The process differentiating U from Pb in the Modum complex certainly did not give special preference to metacarbonate lithologies, nor was it completely uranium selective. This suggests that the process leading to an increased U/Pb ratio is different from that giving high ratios in most limestones or metamorphic marbles, and that it is related to a metamorphic event rather than to pre-metamorphic processes in the sediments. In their study of the distribution of heat-producing elements in granitic rocks of South Norway, Killeen & Heier (1975) observed high U and Th contents in parts of the Levang Gneiss Dome in the Bamble sector, and related this to U and Th introduction during Sveconorwegian metamorphism.

Although uranium has been added to metasediments over large parts of the Sveconorwegian province of South Norway, this is very unlikely to have been due to a single event of fluid-rock interaction, or to fluids emanating from a single source of fluid or of uranium. Most likely, the increase in U/Pb is brought about by a number of individual metasomatic events, which may be closely related in terms of fluid chemistry and physical conditions, but which were neither strictly synchronous nor genetically interrelated over the whole area. Common to these processes over the entire region must have been access to a uniformly distributed reservoir of uranium and thorium, and a fluid capable of mobilizing the elements. Granitic rocks with elevated LILE concentrations may be the most likely source for uranium. At amphibolite-facies pressure and temperature conditions, chloride-bearing aqueous fluids are able to remobilize significant amounts of the uranium bound in zircon (Sinha et al. 1992); this effect may be even stronger for uranium situated at grain boundaries and in less favourable sites in minerals.

In South Norway, uranium may have been remobilized both from pre-Svenconorwegian rocks, such as the basement on which the sedimentary rocks were deposited, and from syn-tectonic Sveconorwegian granitic intrusions, which overlap in age with the uranium introduction to the sediments. The moderate fit to a correlation line with a normal crustal Th/U ratio of 4 in the $^{208}Pb/^{204}Pb$ vs. $^{206}Pb/^{204}Pb$ diagram (Fig. 2c) supports a normal upper crustal source for the trace components introduced.

## Implications for the age and LILE characteristics of the crustal precursor

The single-stage model $\mu_1$ value of $8.20 \pm 0.02$ indicated by the Sveconorwegian Pb–Pb correlation line is high compared to the $^{238}U/^{204}Pb$ of 7.90–7.95 estimated for the mantle source of the Bamble crust (Andersen et al. 1994).The time-integrated model $\mu_1$ value calculated from 1131 Ma correlation line incorporates all stages of the presumably complex evolutionary history of the source terrane prior to this date. In a simplistic extension of the two-stage model, an intermediate reservoir, representing the average crustal source of sedimentary material may be assumed to have formed some time prior to 1131 Ma, to evolve at a given, time-integrated $^{238}U/^{204}Pb$ ratio until 1131 Ma. The simple two-stage model adds the growth in the mantle- and crustal precursor reservoirs together under a single model $\mu_1$ value. A model $\mu_1$ value higher than mantle values indicates that the $^{238}U/^{204}Pb$ of the intermediate resevoir (i.e. the crustal precursor) was elevated compared to the mantle, and that the initial lead of the sediments must have resided in such a reservoir for several hundred million years.

An elevated $^{238}U/^{204}Pb$ ratio suggests that the source terrane(s) of the sediments had a LILE-enriched character, typical of the upper continental crust (e.g. Zartman & Doe 1981). A conservative estimate of the degree of U enrichment of this crustal domain is given by the $^{238}U/^{204}Pb$ ratio needed to reproduce a 1.13 Ga initial lead composition on the overall correlation line from a source extracted from a mantle with $^{238}U/^{204}Pb = 7.9$ (Andersen et al. 1994) at the time of initial formation of the average crustal precursor (Fig. 7). 1.9 Ga is chosen as the age of the crustal precursor, rather than younger values within the range of Nd model ages for these and related rocks (1.7–1.9 Ga; Munz et al. 1994; Andersen et al. 1995) in order to obtain a conservative (i.e. minimum) estimate of its average $^{238}U/^{204}Pb$ ratio. The Pb isotopic composition of the mantle at 1.9 Ga is indicated by an asterisk in Fig. 7. At 1.13 Ga, all crustal systems extracted from this mantle source plot on the 1900 Ma paleoisochron (assuming, of course, that no internal U/Pb differentiation has taken place during the life-time of the crustal reservoir, which is a gross oversimplification). In inset *ii* to Fig. 7, growth curves for model systems with $^{238}U/^{204}Pb = 12$ and 24 are shown. Whereas a $^{238}U/^{204}Pb$ ratio

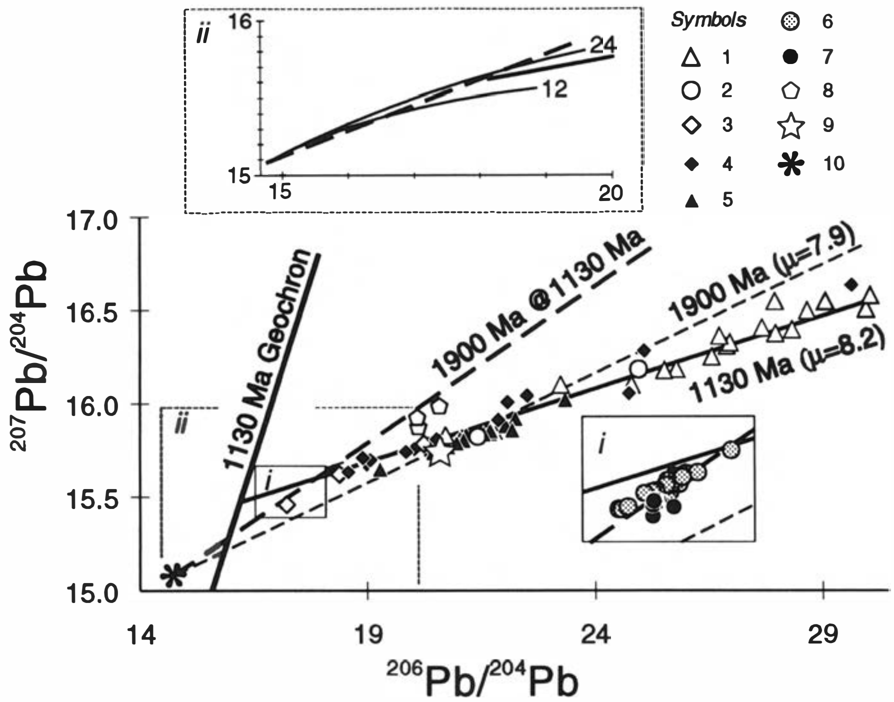


*Fig. 7.* Model of Pb isotopic evolution. *Main diagram symbols*: 1 = Metasedimentary rocks from the Modum complex, 2 = Cordierite-bearing rocks, Bamble sector, 3 = quartzites and metasedimentary gneisses, Bamble sector (Table 1), 4 = quartzites and quartz–sillimanite gneisses, Bamble sector (Andersen et al. 1995), 5 = sulphides from 270 Ma vein deposits, Bamble (Tråk deposits) and Kongsberg sectors (Bjørlykke et al. 1990), 6 = sulphide vein deposits, Dalsland and Värmskog areas, Sweden (Johansson 1985), 7 = Ubergsmoen initial lead (Andersen et al. 1994), 8 = Mn-rich vein deposits, Central South Sweden (Romer & Wright 1993), 9 = South Telemark average crust (Andersen & Taylor 1988), 10 = Theoretical composition of a mantle reservoir with $\mu = 7.9$ at 1900 Ma (see text). *Model isochron lines*: Heavy solid = Geochron at 1130 Ma. Solid = Final stage best-fit reference line (scatterchron), single-stage model $\mu_1 = 8.2$ (cf. Fig. 2a, b). Thin dashed = 1900 Ma isochron (single-stage model $\mu_1 = 7.9$). Heavy dashed = 1900 Ma paleoisochron at 1130 Ma. *Inset* (*i*) shows an expanded detail (solid box), including the initial lead composition of the Ubergsmoen augen gneiss (Andersen et al. 1994) and sulphides from the Dalsland and Värmskog areas, Sweden (Johansson 1985), as well as parts of the 1130 Ma best-fit line, the 1900 Ma reference isochron and the 1900 Ma paleoisochron at 1130 Ma (all with signatures as in the main part of the diagram). *Inset* (*ii*) (dashed box) is an expansion of the main diagram, showing critical second-stage growth curves (thin, curved lines). The 1900 Ma at 1130 Ma paleoisochron (broken line) and the 1130 Ma best-fit line (solid line) are shown. The two second-stage growth curves start from a theoretical mantle initial ($\mu_1 = 7.9$) at 1900 Ma (rosette in main diagram) and have $^{238}U/^{204}Pb$ ($\mu_2$) values of 12 and 24 respectively, as indicated. It should be noted that the $\mu_2 = 12$ growth curve falls short of the 1130 Ma best-fit line, whereas the $\mu_2 = 24$ growth curve intersects the paleoisochron very close to the best-fit line.

of 12 is clearly insufficient to produce lead compositions along the 1.13 Ga correlation line in the 770 Ma considered, the growth curve with $^{238}U/^{204}Pb = 24$ intersects the paleoisochron slightly above its crossing with the 1.13 Ga correlation line, suggesting that $^{238}U/^{204}Pb$ ratios of ca. 20–24 are required. The scatter around the correlation line (reflected by its elevated MSWD) is due to heterogeneities of $^{238}U/^{204}Pb$ within the source terrane, which have not been obliterated by erosion, transport and sedimentation.

The initial lead composition of the Ubergsmoen augen gneiss (Andersen et al. 1994) and galenas analysed from the vein deposits in the Sveconorwegian province of South Sweden (Johansson 1985; Romer & Wright 1993) plot below the present isochron, but close to the 1.9 Ga paleoischron at 1.13 Ga (Fig. 7, inset *i*). This indicates that the pre-Sveconorwegian reservoirs in which those leads evolved were less U enriched than the protoliths of the rocks studied here, but that they may have had a similar average age of crustal residence. On the other hand, the initial lead composition of Sveconorwegian manganese-rich veins hosted in the Trans-Scandinavian Igneous Belt of Central South Sweden (Romer & Wright 1993) is strongly radiogenic, but plots only slightly to the right of the 1900 Ma paleoischron in Fig. 7, suggesting a $^{238}U/^{204}Pb$ ratio above 24 for the source region of the fluids forming these veins.

The galena from the Permian Tråk and Kongsberg deposits (ca. 270 Ma, Bjørlykke et al. 1990) are near colinear with the present metasedimentary gneisses at $^{206}Pb/^{204}Pb$ in the lowermost part of the range of the rocks studied here ($^{206}Pb/^{204}Pb$ = ca. 22, Fig. 7), implying that the lead in those deposits was extracted from a crustal source corresponding in post-Sveconorwegian LILE enrichment to the least uranium enriched of the metasediments studied here, to the average of the source terrane of the sediments, and to the 'South Telemark crustal composite' of Andersen & Taylor (1988).

## Conclusions

Metasedimentary rocks from wide areas of the Sveconorwegian province of South Norway show present-day lead isotopic compositions which are significantly more radiogenic than assumed even for LILE-enriched 'upper continental crust' (as envisaged by e.g. Zartman & Doe 1981). In the $^{207}Pb/^{204}Pb$ vs. $^{206}Pb/^{204}Pb$ diagram, the rocks analysed plot along regional correlation lines with elevated MSWD (scatterchrons) suggesting ages in the range 1060–1262 Ma, with an overall correlation at $1131 \pm 30$ Ma (MSWD = 17.3). This age is interpreted as the age of U/Pb differentiation, without or with incomplete isotopic homogenization of lead. Calculated post-Sveconorwegian $^{238}U/^{204}Pb$ ratios for the rocks studied range from 6 to 554, most samples show calculated $^{238}U/^{204}Pb$ ratios above 24.

This correlation reflects one or more event(s) of metasomatic introduction of uranium (and to some extent thorium) to the metasediments in the Sveconorwegian. Uranium introduction was coupled to imperfect or entirely absent isotopic homogenization of lead. Despite the heterogeneous initial lead isotopic composition in the Sveconorwegian, the large spread in U/Pb allows the calculation of meaningful ages, which suggests that the U-enrichment is coeval with metamorphic episodes of regional singificance.

The source terrane of clastic material was itself LILE enriched, with U/Pb ratios integrated over its lifetime above the average normal upper continental crust. To account for the range in initial lead composition in the Sveconorwegian, the exposed continental crust in the area must have retained a high $^{238}U/^{204}Pb$ ratio for several hundred million years. Assuming that the average crustal protolith was extracted from the mantle at 1.7–1.9 Ga, time- and area-integrated $^{238}U/^{204}Pb$ ratios in the range 20–24 may be estimated; if the protolith is younger, the average $^{238}U/^{204}Pb$ ratio must have been correspondingly higher.

The source terrane of sediments in the Bamble and Kongsberg sectors may possibly correspond to ca. 1.76 Ga or older crustal segments further to the east, bordering on the main Svecofennian continent, such as the Østfold–Marstrand belt (Åhäll & Daly 1989). The U–Pb characteristics of metasupracrustals in this crustal segment will be the subject of a subsequent study.

*Acknowledgements.* – The laboratory work was supported by grants from Norges Forskningsråd (previously NAVF) to Tom Andersen and to the Laboratory of Isotope Geology at the Mineralogical–Geological Museum, University of Oslo. We thank Jan Kihle, Lars Kullerud and Karl-Inge Åhäll for providing samples from the Bamble sector, and Martin Whitehouse, Håkon Austrheim, Jacques Touret, Bjørn Sundvoll, Kees Maijer and Rob Verschure for numerous helpful discussions on South Norway and its isotope geology. The manuscript benefited from helpful reviews by Stephen Moorbath, Stefan Claesson and N.N.

Manuscript received February 1995

# References

Åhäll, K. I. & Daly, J. S. 1989: Age, tectonic setting and provenance of Östfold–Marstrand Belt supracrustals: westward crustal growth of the Baltic Shield at 1760 Ma. *Precambrian Research 45*, 45–61.

Andersen, T., Hagelia, P. & Whitehouse, M. J. 1994: Precambrian multi-stage crustal evolution in the Bamble sector of S. Norway: Pb isotopic evidence from a Sveconorwegian deep-seated granitic intrusion. *Chemical Geology (Isotope Geosciences Section) 116*, 327–343.

Andersen, T., Maijer, C. & Verschure, R. H. 1995: Metamorphism, provenance ages and source characteristics of Precambrian clastic sediments in the Bamble Sector, South Norway: An Ar, Sr, Nd and Pb isotope study. *Petrology (Moscow)*. In press.

Andersen, T. & Taylor, P. N. 1988: Lead isotope geochemistry of the Fen carbonatite complex, S.E. Norway: age and petrogenetic implications. *Geochimica et Cosmochimica Acta 52*, 209–215.

Bjørlykke, A., Ihlen, P. M. & Olerud, S. 1990: Metallogeny and lead isotope data from the Oslo Paleorift. *Tectonophysics 178*, 109–126.

Brøgger W. C. 1934: On several Archaean rocks from the South coast of Norway. I. Nodular granites from the environs of Kragerø. *Skrifter, Det Norske Videnskaps-Akademi i Oslo, m* 1. *Matem.-Naturvid, Kl. 1993 No. 8.*

Bugge, A. 1936: Kongsberg–Bamble formasjonen. *Norges Geologiske Undersøkelse 146.*

Bugge, A. 1937: Flesberg og Eiker, beskrivelse til de geologiske karter F35Ø og F35V. *Norges Geologiske Undersøkelse 143.*

Bugge, J. A. W. 1943 Geological and petrological investigations in the Kongsberg–Bamble formation. *Norges Geologiske Undersøkelse 160*, 150 pp.

Cameron, E. M. 1989a: Scouring of gold from the lower crust. *Geology 17*, 26–29.

Cameron, E. M. 1989b: Derivation of gold by oxidative metamorphism of a deep ductile shear zone; Part 2, evidence from the Bamble Belt, South Norway. *Journal of Geochemical Exploration 31*, 149–169.

Cameron, E. M. 1993: Reintroduction of gold, other chalcophile elements and LILE during retrogression of depleted granulite, Tromøy, Norway. *Lithos 29*, 303–309.

Cameron, E. M., Cogulu, E. H. & Stirling, J. 1993: Mobilization of gold in the deep crust: evidence from mafic intrusions in the Bamble belt, Norway. *Lithos 30*, 151–166.

Dahlgren, S. H., Heaman, L. & Krogh, T. E. 1990a: Geological evolution and U–Pb geochronology of the Proterozoic central Telemark area, Norway (abstract). *Geonytt 17*, 1:38.

Dahlgren, S., Heaman, L. & Krogh, T. E. 1990b: U–Pb dating of coronitic metagabbros, hornblende–phlogopite–apatite pegmatites and albitites in the Proterozoic Bamble shear belt, South Norway (abstract). *Abstracts, Second Symposium on the Baltic Shield, Lund, Sweden, June 1990.*

De Haas, G-J. L. M., Verschure, R. H. & Maijer, C. 1993: Isotopic constraints on the timing of crustal accretion of the Bamble sector, Norway, as evidence by coronitic gabbros. *Precambrian Research 64*, 403–417.

DePaolo, D. J. 1981: Neodymium isotopes in the Colorado Front Range and crust-mantle evolution in the Proterozoic. *Nature 291* 193–196.

Elliot, R. B. & Morton, R. D. 1965: The nodular metamorphic rocks from the environments of Kragerö, south coast of Norway. *Norges Geologiske Undersøkelse 45*, 1–20.

Faure, G. 1977: *Principles of Isotope Geology*, 1st ed. J. Wiley, New York. 464 pp.

Faure, G. 1986: *Principles of Isotope Geology*, 2nd ed. J. Wiley, New York. 589 pp.

Field, D., Drury, S. A. & Cooper, D. C. 1980: Rare-earth and LIL element fractionation in high-grade charnockitic gneisses, south Norway. *Lithos 13*, 281–289.

Field, D., Smalley, P. C., Lamb, R. C. & Råheim, A. 1985: Geochemical evolution of the 1.6–1.5 Ga-old amphibolite–granulite facies terrain, Bamble Sector, Norway: Dispelling the myth of Grenvillian high-grade reworking. *In* Tobi, A. C. & Touret, J. (eds): *The Deep Proterozoic Crust in the North Atlantic Provinces*, 567–578. NATO ASI Series C 158. Reidel, Dordrecht.

Gaál, G. & Gorbatschev, R. 1987: An outline of the Precambrian evolution of the Baltic Shield. *Precambrian Research 35*, 15–52.

Gale, N. H. & Mussett, A. E. 1973: Episodic uranium–lead models and the interpretation of variations in the isotopic composition of lead in rocks. *Reviews of Geophysics and Space Physics 11, No. 1*, 37–86.

Gorbatschev, R. & Bogdanova, S. 1993: Frontiers in the Baltic Shield. *Precambrian Research 64*, 3–21.

Hagelia, P. 1989: Structure, metamorphism and geochronology of the Skagerrak shear belt, as revealed by studies in the Hovdefjell–Ubergsmoen area, South Norway. Unpublished cand. scient. thesis, University of Oslo 236 pp.

Heaman, L. M. & Smalley, P. C. 1994: A U–Pb study of the Morkheia Complex and associated gneisses, southern Norway: implications for disturbed Rb–Sr systems and for the temporal evolution of Mesoproterozoic magmatism in Laurentia. *Geochimica et Cosmochimica Acta 58*, 1899–1911.

Hemming S. R., McLennan, S. M. & Hanson, G. N. 1994: Lead isotopes as a provenance tool for quartz: examples from plutons and quartzite, Northeastern Minnesota, USA. *Geochimica et Cosmochimica Acta 58*, 4455–4464.

Jacobsen, S. & Heier, K. S. 1978: Rb–Sr systematics in metamorphic rocks, Kongsberg sector, South Norway. *Lithos 11* 257–276.

Jahn, B.-m. & Cuvellier, H. 1994: Pb–Pb and U–Pb geochronology of carbonate rocks: an assessment. *Chemical Geology 115*, 125–151.

Johansson, Å, 1985: The Dalslandian sulphide-bearing quartz veins of Dalsland and Värmskog Southwest Sweden. *Sveriges Geologiska Undersökning C809*, 48 pp.

Jøsang, O. 1966: Geologiske og petrografiske undersøkelser i Modumfeltet. *Norges Geologiske Undersøkelse 235*, 148 pp.

Kihle. J. 1989: Polymetamorf utvikling av cordieritt-førende metapelitter i Bamblesektoren, Syd-Norge. Unpublished Cand. Scient. thesis, University of Oslo 360 pp.

Kihle, J. & Bucher-Nurmien, K. 1992: Orthopyroxene–sillimanite–sapphirine granulites from the Bamble granulite terrain, southern Norway. *Journal of Metamorphic Geology 10*, 671–683.

Killeen, P. G. & Heier, K. S. 1975: Radioelement distribution and heat production in Preambrian granitic Rocks, Southern Norway. *Det Norske Videnskaps-Akademi I Mat.-Naturv. Klasse. Skrifter, Ny serie No. 35.*

Knudsen, T.-L. 1995: Fluid–rock interaction during granulite-facies metamorphism of metapelites from the Proterozoic lower crust in the Hisøy-Torungen area, Bamble sector, Southern Norway. Manuscript in prep.

Kullerud, L. 1991: Gjeving charnockite. Excursion log to the 2nd SNF Workshop, Bamble (unpublished). 70–71.

Kullerud, L. & Dahlgren, S. H. 1993: Sm–Nd geochronology of Sveconorwegian granulite-facies mineral assemblages in the Bamble Shear Belt, South Norway. *Precambrian Research 64*, 389–402.

Kullerud, L. & Machado, N. 1991: End of a controversy: U–Pb geochronological evidence for significant Grenvillian activity in the Bamble area, Norway. *Terra Abstracts 3*, 504.

Lambert, I. B. & Heier, K. S. 1967: The vertical distribution of uranium, thorium and potassium in the continental crust. *Geochimica et Cosmochimica Acta 31*, 377–390.

Ludwig, T. C. 1986: ISOPLOT200: A plotting and regression program for isotope geochemists, for use with HP Series 200 computers. *United States Geological Survey Open File Report 85-513.*

Moorbath, S. & Vokes, F. M. 1963: Lead isotope abundance studies on galena occurrences in Norway. *Norsk Geologisk Tidsskrift 43*, 283–343.

Munz, I. A. 1986: Geologisk utvikling av Modumfeltet, med vekt på den metamorfe historie. Unpublished Cand. Scient. Thesis, University of Oslo.

Munz, I. A. 1990: Whiteschists and orthoamphibole–cordierite rocks and the P-T-t path of the Modum Complex, South Norway. *Lithos 24*, 181–200.

Munz, I. A. & Morvik, R. 1991: Metagabbros in the Modum Complex, southern Norway: an important heat source for Sveconorwegian metamorphism. *Precambrian Research 52*, 97–113. Corrigendum: *Precambrian Research 53*, 305.

Munz, I. A., Wayne, D. & Austrheim, H. 1994: Retrograde fluid infiltration in the high-grade Modum Complex, South Norway: evidence for age, source and REE mobility. *Contributions to Mineralogy and Petrology 116*, 32–46.

Munz, I. A., Yardley, B. W. D., Banks, D. A. & Wayne, D, 1995: Deep penetration of sedimentary fluids in basement rocks from southern Norway: evidence from hydrocarbon and brine inclusions in quartz veins. *Geochimica et Cosmochimica Acta 59*, 239–254.

Nijland, T. G. 1993: The Bamble amphibolite to granulite facies transition zone, Norway. *Geologica Ultraiectina 101*, 166 pp.

Nijland, T. G. Maijer, C., Senior A. & Verschure, R. H. 1993: Primary sedimentary structures and compositions of the high-grade metamorphic Nidelva Quartzite Complex (Bamble, Norway) and the origin of nodular gneisses. *Koninglijke Nederlandse Akadademie van Wetenschappen, Proceedings 96*, 217–232.

O'Nions, R. K. & Baadsgaard, H. 1971: A radiometric study of the polymetamorphism in the Bamble region, Norway. *Contributions to Mineralogy and Petrology 34*, 1–21.

Petrascheck, L. 1971: Der kristalline Magnesit in Serpentin von Snarum (Norwegen). *Radex-Rundschau*, Heft 3, 487–491.

Romer, R. E. & Wright, J. E. 1993: Lead mobilization during tectonic reactivation of the western Baltic shield. *Geochimica et Cosmochimica Acta 57*, 255–257.

Rosholt, J. N. & Noble, D. C. 1969: Loss of uranium from crystallised silicic volcanic rocks. *Earth and Planetary Science Letters 6*, 268–270.

Rosholt, J. N., Zartman, R. E. & Nkomo, I. T. 1973: Pb-isotope systematics and uranium depletion in the Granite Mountains, Wyoming. *Geological Society of America Bulletin 84*, 989–1002.

Sinha, A. K., Wayne, D. M. & Hewitt, D. A. 1992: The hydrothermal stability of zircon: preliminary experimental and isotope studies. *Geochimica et Cosmochimica Acta 56*, 3551–3560.

Smalley, P. C., Field, D., Lamb, R. C. & Clough, P. W. L. 1983: Rare earth, Th–Hf–Ta and large ion lithophile element variations in metabasites from the Proterozoic amphibolite–granulite transition zone at Arendal, South Norway. *Earth and Planetary Science Letters 63*, 446–458.

Starmer, I. C. 1976: The early major structure and petrology of the rocks in the Bamble series, Søndeled–Sandnesfjord, Aust-Agder, *Norges Geologiske Undersøkelse Bulletin 338*, 37–58.

Starmer, I. C. 1985: The evolution of the South Norwegian Proterozoic as revealed by the major and mega-tectonics of the Kongsberga and Bamble sectors. *In* Tobi, A. C. & Touret, J. L. R. (eds): *The Deep Proterozoic Crust in the North Atlantic Provinces*, 259–290. D. Reidel, Dordrecht.

Sundvoll, B. & Larsen, B. T. 1993: Rb–Sr and Sm–Nd relationship in dyke and sill intrusions in the Oslo Rift and related areas. *Norges Geologiske Undersøkelse Bulletin 425*, 31–42.

Taylor, S. R. & McLennan, S. M. 1985: *The Continental Crust: Its Composition and Evolution.* Blackwell, Oxford. 312 pp.

Thijssen, P. H. M. & Maijer, C. 1990: Sapphirine paragenesis from Snaresund, Bamble, Norway. *Geonytt 17*, 114.

Touret, J. L. R. 1969: Le socle Précambrien de la Norvège méridionale (Région de Vegårshei-Gjerstad). Unpublished PhD thesis, University of Nancy, CNRS no.AO 2902, 316 pp.

Touret, J. L. R. 1971a; Le faciès granulite en Norvèges méridionale. I Les associations minéralogiques. *Lithos 4*, 239–249.

Touret, J. L. R. 1971b: Le facies granulite en Norvège méridionale, II: les inclusions fluides. *Lithos 4*, 423–436.

Touret, J. L. R. 1985: Fluid regime in Southern Norway: The record of fluid inclusions. *In* Tobi, A. C. & Touret, J. L. R. (eds): *The Deep Proterozoic Crust in the North Atlantic Provinces*, 517–550. D. Reidel, Dordrecht.

Visser, D. 1993: The metamorphic evolution of the Bamble sector, South Norway: a paragenetic and mineral chemical study of cordierite–orthoamphibole–bearing rocks with special reference to borosilicate-bearing mineral assemblages. *Geologica Ultraiectina 103.*

Whitehouse, M. J. 1989: Pb-isotope evidence for U–Th–Pb behaviour in a prograde amphibolite to granulite facies transition from the Lewisian complex of north-west Scotland: implications for Pb-Pb dating. *Geochimica et Cosmochimica Acta 53*, 717–724.

Zartman, R. A. & Doe, B. R. 1981: Plumbotectonics – the model. *Tectonophysics 75*, 135–162.